arXiv:1606.03250v1 [hep-ph] 10 Jun 2016

HYDRO + JETS (HYDJET++) event generator for Pb+Pb collisions at LHC

L Bravina[1,4,5], B H Brusheim Johansson[1], J Crkovská[3], G Eyyubova[2], V Korotkikh[2], I Lokhtin[2], L Malinina[2], E Nazarova[2], S Petrushanko[2], A Snigirev[2], E Zabrodin[1,2,4,5]

[1] Department of Physics, University of Oslo, Norway
[2] Skobeltsyn Institute of Nuclear Physics, Lomonosov Moscow State University, Moscow, Russia
[3] Institut de Physique Nucléaire, CNRS-IN2P3, Univ. Paris-Sud, Université Paris-Saclay, France
[4] Frankfurt Institute for Advanced Studies, D-60438 Frankfurt a.M., Germany
[5] National Research Nuclear University "MEPhI" (Moscow Engineering Physics Institute), Moscow, Russia

E-mail: larissa.bravina@fys.uio.no

Abstract. The Monte Carlo event generator HYDJET++ is one of the few generators, designed for the calculations of heavy-ion collisions at ultrarelativistic energies, which combine treatment of soft hydro-like processes with the description of jets traversing the hot and dense partonic medium. The model is employed to study the azimuthal anisotropy phenomena, dihadron angular correlations and event-by-event (EbyE) fluctuations of the anisotropic flow in Pb+Pb collisions at $\sqrt{s_{\rm NN}} = 2.76$ TeV. The interplay of soft and hard processes describes the violation of the mass hierarchy of meson and baryon elliptic and triangular flows at $p_{\rm T} \geq 2$ GeV/c, the fall-off of the flow harmonics at intermediate transverse momenta, and the worsening of the number-of-constituent-quark (NCQ) scaling of elliptic/triangular flow at LHC compared to RHIC energies. The cross-talk of v_2 and v_3 leads to emergence of higher order harmonics in the model and to appearance of the *ridge* structure in dihadron angular correlations in a broad pseudorapidity range. HYDJET++ possesses also the dynamical EbyE fluctuations of the anisotropic flow. The model results agree well with the experimental data.

1. Introduction. HYDJET++ model

The Monte Carlo event generator HYDJET++ (HYDrodynamics with JETs) [1] consists of two parts describing the soft and the hard processes, respectively. The generator of soft processes FASTMC [2] was originally designed to help the experimentalists in simulation of significant data samples of heavy-ion collisions at energies of RHIC and LHC. The demands to the model were formulated as follows: (i) it should be able to simulate tens of thousands of central gold-gold or lead-lead events at energies from $\sqrt{s_{\rm NN}} = 200$ GeV to several TeV within relatively modest CPU time; (ii) the yields and transverse momentum spectra of most abundant particles should be very close to real data. To meet these requirements the authors opted for parameterised ideal hydrodynamics. The model was extended soon to non-central nuclear interactions [3]. The first step is the calculation of the effective volume of the fireball $V_{\rm eff}$ which is a subject of the mean number of participating nucleons at given collision centrality. Particle composition

is frozen at chemical freeze-out, but the fireball expands further and breaks down at thermal freeze-out temperature, where the contact between hadrons is lost. The final-state interactions (FSI) assume two- and three-body decays of resonances. The table of particles in the model contains more than 360 meson and baryon states including also the charmed ones. This approach is close to the THERMINATOR model [4]. Obviously, the ideal hydrodynamic description of particle spectra is justified for transverse momenta below 2 GeV/c. At higher $p_{\rm T}$ one has to take into account hard processes. These processes are governed by the PYQUEN routine [5], which propagates the hard partons through the hot and dense medium, most presumably quark-gluon plasma. The partons experience collisional and radiative energy losses. At the end of the rescattering stage all emitted quarks and gluons are hadronized according to the Lund model. The number of produced jets in HYDJET++ is proportional to the number of binary nucleon-nucleon collisions at a given impact parameter and the integral cross section of the hard processes in NN collision with minimal transverse momentum transfer.

The synergy between the soft processes and quenched jets became obvious soon after the merging of two independent generators, FASTMC and PYQUEN, into the model called HYDJET++ [1]. Several examples concerning the interplay of hard and soft processes will be discussed in Sec. 2. Then, the model was further upgraded. Namely, after the publication of first data on proton-proton collisions at $\sqrt{s_{\rm NN}} = 7$ TeV it became clear that the standard version of PYTHIA_6.4 [6] should be adjusted. Several tunes have been proposed and the HYDJET++ group has opted for Pro-Q20 tune in the new release of the model [7]. Next was the extension of the model to triangular flow [8].

Recall that the azimuthal distribution of particles can be cast [9, 10] in the form of Fourier series

$$E\frac{d^3N}{d^3p} = \frac{1}{2\pi}\frac{d^2N}{p_{\rm T}dp_{\rm T}dy}\left\{1 + \sum_{n=1}^{\infty} 2v_n \cos\left[n(\phi - \Psi_n)\right]\right\} \ . \tag{1}$$

Here ϕ, $p_{\rm T}$ and y are the azimuthal angle, the transverse momentum and the rapidity of a particle, respectively. Ψ_n is the azimuth of the corresponding event plane, and the sum of harmonics in the rhs of Eq. (1) represents anisotropic flow. The coefficients v_n are dubbed directed flow v_1, elliptic flow v_2, triangular flow v_3 and so forth. In HYDJET++ elliptic and triangular flows arise because of the corresponding spatial eccentricities of the fireball. The radii of the elliptic and triangular spatial eccentricities are defined as function of the impact parameter b and azimuthal angle ϕ as follows [3, 8] :

$$R_{\rm ell}(b,\phi) = R_{\rm fr}\left[\frac{1-\varepsilon^2(b)}{1+\varepsilon^2(b)\cos 2(\phi-\Psi_2)}\right]^{1/2} , \tag{2}$$

$$R_{\rm trian}(b,\phi) = R_{\rm ell}(b,\phi)\{1+\varepsilon_3(b)\cos 3(\phi-\Psi_3)\} , \tag{3}$$

where $R_{\rm fr}(b) = R_0\sqrt{1-\varepsilon(b)}$, and R_0 is the freeze-out radius of the fireball in a central collision. Two free parameters, $\varepsilon(b)$ and $\varepsilon_3(b)$, control the ellipticity and triangularity of the fireball. Ψ_2 and Ψ_3 are the azimuths of the corresponding event planes randomly distributed with respect to each other. The pressure gradients are stronger in the direction of short axis of the ellipsoid, however, the momentum anisotropy angle $\phi_{\rm fl}$ is related to the spatial anisotropy ϕ via

$$\frac{\tan\phi_{\rm fl}}{\tan\phi} = \left[\frac{1-\delta(b)}{1+\delta(b)}\right]^{1/2} , \tag{4}$$

containing the third (and the last) free parameter, $\delta(b)$, responsible for the formation of anisotropic flow in HYDJET++. The cross-talk of elliptic and triangular harmonics leads to appearance of both even and odd higher harmonics of the anisotropic flow in the model because

of the nonlinear contributions to v_n from v_2, v_3 or their product $v_2 v_3$. This interplay explains also the formation of ridge in long-range dihadron correlations, including the characteristic double-bump profile of the ridge at the away-side [11]. The last developments of the model deal with its extension to open and hidden charm production [12] and to EbyE fluctuations of the anisotropic flow [13]. The aspects of the calculations are presented in Sec. 2. Conclusions are drawn in Sec. 3.

2. Interplay of soft processes, jets and final-state interactions

Consequences for elliptic and triangular flows. Hadrons produced in soft processes at the freeze-out hypersurface should carry collective flow, whereas the flow assigned to jet particles with intermediate transverse momenta is essentially zero. At $p_{\rm T} \geq 4$ GeV/c hadrons decoupled from jets can develop a weak anisotropic flow because of the well-known effect of jet quenching. Decays of resonances also modify the $p_{\rm T}$ distributions of the flow excitation functions. In HYDJET++ these effects were studied in non-central heavy-ion collisions at RHIC and LHC energies in [14, 15] for the elliptic flow and in [16, 17] for the triangular flow, respectively.

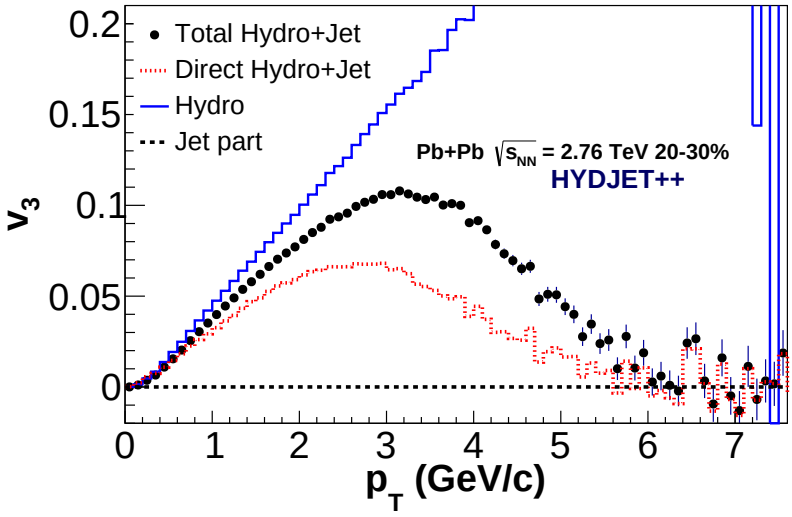

Figure 1. The $p_{\rm T}$ dependence of the triangular flow of charged particles produced in soft+hard (circles) and soft processes (solid line), from the jets (dashed line) and direct particles (dotted line) in HYDJET++ in Pb + Pb collisions at $\sqrt{s_{\rm NN}} = 2.76$ TeV at centrality 20-30%.

To illustrate the typical features of the development of the flow components we plot in Fig. 1 triangular flow of charged hadrons produced in Pb+Pb collisions at $\sqrt{s_{\rm NN}} = 2.76$ TeV at centrality $\sigma/\sigma_{geo} = 20 - 30\%$. The partial flow of jet hadrons is absent, while the flow of particles governed by hydrodynamics increases with rising $p_{\rm T}$. Hadrons from the soft processes dominate the particle spectrum at $p_{\rm T} \leq 2$ GeV/c, and the total v_3 increases in this $p_{\rm T}$ range. At higher transverse momenta the fraction of jet hadrons prevails over the "soft" ones. Thus, the triangular flow in HYDJET++ decreases after a certain $p_{\rm T}$. The lighter the hadron, the smaller is the value of transverse momentum where the spectra of hadrons originated from the soft and the hard processes cross each other. This circumstance explains the violation of the mass ordering of hadron elliptic and triangular flows. One can also see in Fig. 1 that the decays of resonances increase the maximum of the $v_3(p_{\rm T})$ distribution by about 20% and shift its position to higher $p_{\rm T}$. However, 90% of hadrons have the transverse momenta less than 1 GeV/c; therefore, the $p_{\rm T}$-integrated values of v_3 at selected centralities are changed insignificantly [17].

Another important result of the interplay of soft and hard processes is the worsening of the number-of-constituent-quark (NCQ) scaling for both elliptic and triangular flow at LHC energies compared to the RHIC ones. The $v_2(KE_T/n_q)/n_q$ distributions of most abundant hadron species, where $KE_T = m_T - m_0$ is the transverse kinetic energy and n_q is the number of constituent quarks, are shown in Fig. 2. Experimental results of ALICE collaboration [18] are plotted onto the calculations as well. We see that the model provides a fair description of the data.

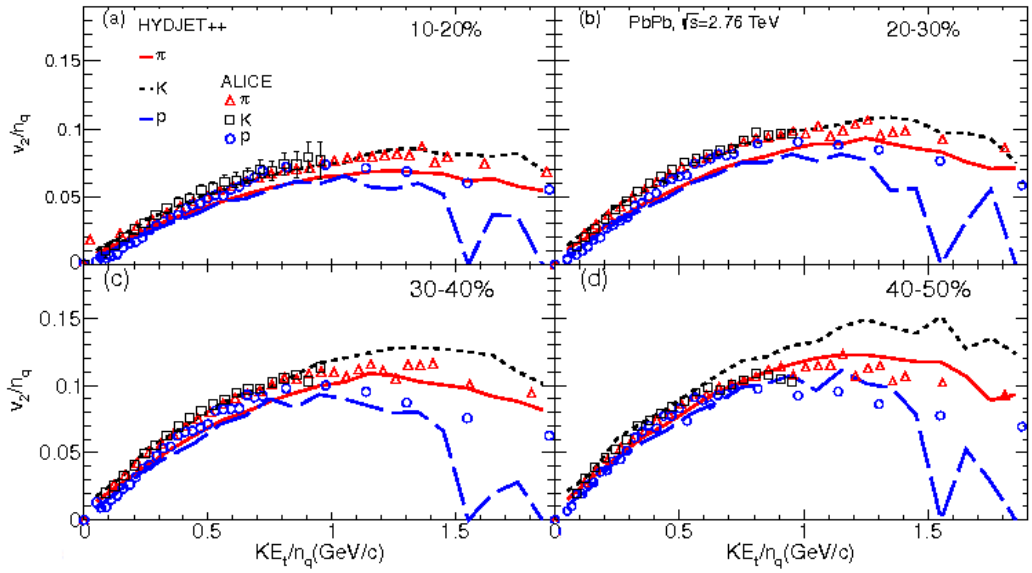

Figure 2. The KE_T/n_q dependence of elliptic flow of pions, kaons and protons in Pb+Pb collisions at $\sqrt{s_{NN}} = 2.76$ TeV at different centralities. Curves denote the model results, ALICE data from [18] are shown by symbols.

The scaling is approximately fulfilled within the 20% accuracy limit in the interval $0.1 \leq KE_T \leq 0.7$ GeV. The worsening of the NCQ scaling conditions for v_2 at LHC was predicted in HYDJET++ in [14, 15]. Our study shows that the effect takes place for both v_2 [14, 19] and v_3 [16, 17] distributions. Scaling definitely holds in the hydrodynamic sector of the model. Moreover, FSI work towards its fulfilment, because many light hadrons, especially pions, get the feeddown from the decays of heavy resonances. But jets, which are more influential at LHC energies compared to that of RHIC, is the main reason causing the NCQ-scaling violation with increasing collision energy.

Cross-talk of elliptic and triangular flows. The present version of HYDJET++ contains no genuine flow harmonics related to the eccentricities of order higher than three. Higher flow harmonics v_n, $n \geq 4$ arise due to nonlinear contributions of v_2 and v_3 [8, 20]. The detailed comparison of model predictions with the data shows [8] that HYDJET++ underpredicts the magnitude of $v_4(p_T)$ - $v_6(p_T)$ signals in central events 0-5%, but for more peripheral collisions the agreement between the model results and the data is much better. It means that nonlinear contributions of v_2 and v_3 to higher harmonics dominate over the intrinsic momentum anisotropy v_n caused by spatial eccentricity ε_n. Of particular interest is the hexagonal flow v_6, because in pure hydrodynamic approximation this harmonic depends on independent contributions coming

from v_2 and v_3 [20]:

$$v_6 \approx \frac{1}{6}v_2^3 + \frac{1}{2}v_3^2 \tag{5}$$

The ratio $v_n^{1/n}/v_2^{1/2}$ was proposed in [21] to check the possible scaling trends. We employed this ratio for the hexagonal flow, and used the v_6 defined either in Ψ_2 or Ψ_3 plane, but not in the own Ψ_6 plane. Results [20] are displayed in Fig. 3 for $v_6^{1/6}/v_2^{1/2}$ and in Fig. 4 for $v_6^{1/6}/v_3^{1/3}$ distributions.

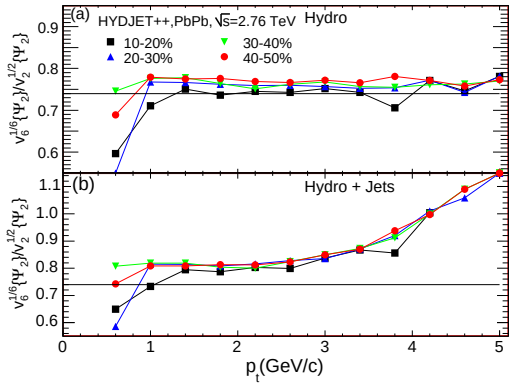

Figure 3. (a) Ratio $v_6^{1/6}/v_2^{1/2}$ in the Ψ_2 event plane for charged hadrons from soft processes calculated in HYDJET++ for Pb+Pb collisions at 2.76 TeV at several centralities. (b) The same as (a) but for both soft and hard processes.

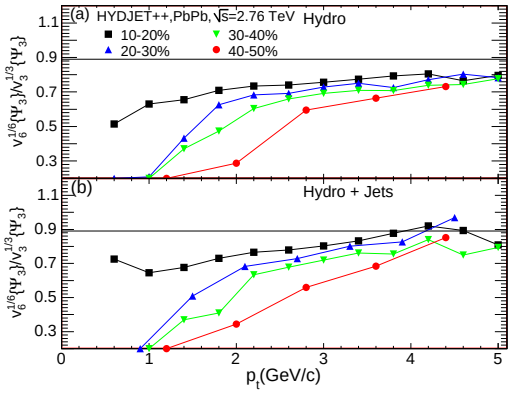

Figure 4. (a) Ratio $v_6^{1/6}/v_3^{1/3}$ in the Ψ_3 event plane for charged hadrons from soft processes calculated in HYDJET++ for Pb+Pb collisions at 2.76 TeV at several centralities. (b) The same as (a) but for both soft and hard processes.

For the $v_6^{1/6}/v_2^{1/2}$ distributions in Fig. 3 the independence of the ratio on centrality of the collision is observed at $p_{\rm T} \geq 1$ GeV/c. All curves are on the top of each other. For the particles produced solely in soft processes this ratio is indeed close to $(1/6)^{1/6}$, whereas jets increase it by about 10% and lead to the rise of high-$p_{\rm T}$ tails of the distributions at $p_{\rm T} \geq 3$ GeV/c. For the $v_6^{1/6}/v_3^{1/3}$ ratios the centrality hierarchy is revealed instead of the scaling. Here the ratio drops as the reactions become more peripheral. This may be explained by the significant rise of the elliptic flow with increasing impact parameter b, while the rise of the triangular flow in more peripheral collisions is not so dramatic. As a result, the event plane Ψ_6 becomes more correlated with the plane Ψ_2 rather than with Ψ_3. This is in line with the experimental observations [22].

Next interesting issue is the study of two-particle angular correlations. The two-particle correlation function is typically defined as the ratio of pair distribution in the event to the combinatorial background of uncorrelated particles. In the flow dominated regime the pair angular distribution reads [cf. Eq.(1)]

$$\frac{dN^{pairs}}{d\Delta\varphi} \propto 1 + 2\sum_{n=1}^{\infty} V_n(p_{\rm T}^{\rm tr}, p_{\rm T}^{\rm a}) \cos n(\Delta\varphi) \ , \tag{6}$$

where $\Delta\varphi = \varphi^{\rm tr} - \varphi^{\rm a}$, and indices "tr" and "a" indicate the so-called "trigger" and "associated" particle, respectively. The study of angular dihadron correlations in relativistic heavy-ion collisions revealed the long-range correlations dubbed "ridge" [23, 24]. Many interesting options have been proposed for the description of the ridge phenomenon, for instance Cerenkov gluon

radiation or Mach-cone of shock waves. The authors of [25] suggested that the triangular flow should be important for understanding of this signal. HYDJET++ is ideally suited for such a check, because the long-range correlations in the model appear merely due to the collective flow.

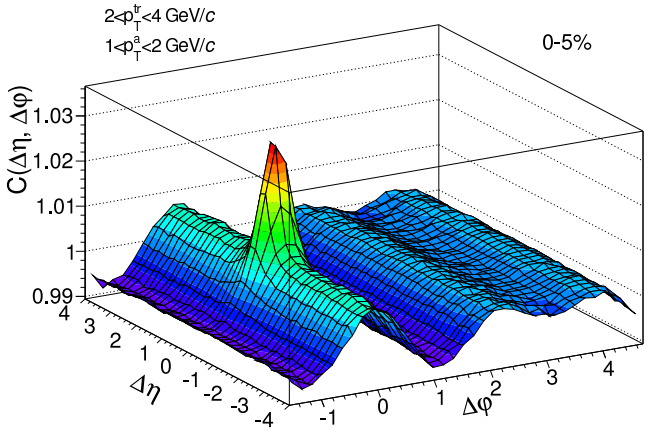

Figure 5. 2D correlation function in HYDJET++ in Pb+Pb collisions at $\sqrt{s} = 2.76$ TeV for $2 < p_{\rm T}^{\rm tr} < 4$ GeV/c and $1 < p_{\rm T}^{\rm a} < 2$ GeV/c for centrality 0-5% with both v_2 and v_3 present.

As was shown in [11], no long range azimuthal correlations at the near-side or away-side ($\Delta\varphi \approx \pi$) appear in the case of perfect central collision with $b = 0$, when both elliptic and triangular flows are absent. If only the elliptic flow is present, whereas the triangular flow is switched off, the long range correlations start to appear at the both sides. However, only the presence of the triangular flow in addition to the elliptic one leads to development of ridge at near-side and, simultaneously, to formation of characteristic double-hump structure at the away-side, as seen in Fig. 5, in full agreement with the experimental observations.

Event-by-Event (EbyE) fluctuations. The EbyE distributions of harmonics of anisotropic flow in lead-lead collisions at LHC were studied, e.g., by ATLAS Collaboration in [26]. The results were obtained after the application of the so-called *unfolding* procedure [27] in order to extract the "true" value of the flow vector and get rid of the nonflow effects caused by the finite event multiplicities, jet fragmentation and decays of resonances. The procedure is cumbersome, so often people simply rescale their predictions to make a comparison with the data. Our analysis shows [13] that such a simplistic approach is not always justified.

As an input, one selects the spectra of charged particles with $p_{\rm T} \geq 0.5$ GeV/c and $|\eta| < 2.5$, corresponding to ATLAS kinematic cuts. Angular distribution of particles is modified as

$$\frac{dN}{d\varphi} \propto 1 + 2\sum_{n=1}^{\infty} V_n^{\rm obs} \cos\left[n(\varphi - \Psi_n^{\rm obs})\right] = 1 + 2\sum_{n=1}^{\infty}\left(V_{n,x}^{\rm obs}\cos n\varphi + V_{n,y}^{\rm obs}\sin n\varphi\right) \ , \qquad (7)$$

with $V_n^{\rm obs}$ being the magnitude of the observed per-particle flow vector, whereas $\Psi_n^{\rm obs}$ represents the azimuth of the observed event plane. Then, the single-particle event-by-event distributions are constructed

$$\begin{aligned} V_n^{\rm obs} &= \sqrt{(V_{n,x}^{\rm obs})^2 + (V_{n,y}^{\rm obs})^2} \ , \\ V_{n,x}^{\rm obs} &= V_n^{\rm obs}\cos n\Psi_n^{\rm obs} = \langle \cos n\varphi \rangle \ , \\ V_{n,y}^{\rm obs} &= V_n^{\rm obs}\sin n\Psi_n^{\rm obs} = \langle \sin n\varphi \rangle \ . \end{aligned} \qquad (8)$$

The two sub-events (2SE) method subdivides the event sample further into two sub-groups containing charged particles emitted in forward and backward hemispheres in the c.m. system.

The difference between the EbyE flow vectors (to exclude the collective flow) of the two sub-events is fitted to the Gaussian with the width $\delta_{\rm 2SE} = 2\delta$, which enters the response function [26]

$$P(V_n^{\rm obs}|V_n) \propto V_n^{\rm obs} \exp\left[-\frac{(V_n^{\rm obs})^2 + V_n^2}{2\delta^2}\right] I_0\left(\frac{V_n^{\rm obs} V_n}{\delta^2}\right) . \quad (9)$$

The obtained response function is then used as an input to the iteration procedure [27] allowing us to find the Bayesian unfolding. The effects of finite multiplicity and nonflow processes give rise to the nonzero value of $\delta_{\rm 2SE}$. The EbyE unfolding procedure significantly subtracts these contributions and leave the dynamical flow fluctuations only.

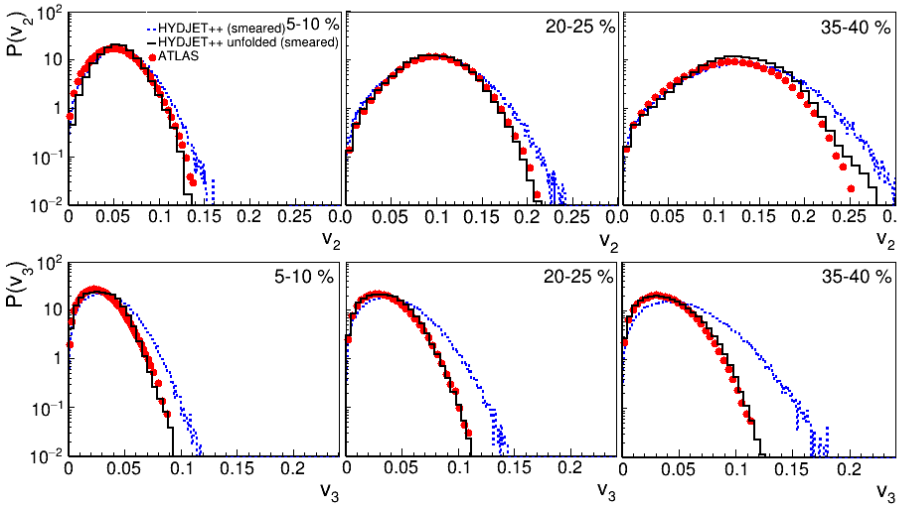

Figure 6. The probability density distributions of elliptic flow V_2 (upper row) and triangular flow V_3 (bottom row) in three centrality intervals: $5-10\%$ (left), $20-25\%$ (middle) and $35-40\%$ (right). Dashed and solid histograms present the results for simulated HYDJET++ events before and after the unfolding procedure, respectively. The full circles are the ATLAS data from [26].

Figure 6 displays the probability density distributions of elliptic and triangular EbyE flows obtained in three centrality intervals: $\sigma/\sigma_{geo} = 5-10\%$, $20-25\%$, and $35-40\%$. To describe the data we allow for variations of $\varepsilon(b)$ and $\varepsilon_3(b)$ [13]. Now the values of both parameters are smeared normally around their previously fixed values. The width proportionality coefficients are tuned to fit the data at a *single arbitrary centrality*, say $10-15\%$ or $20-25\%$, and the obtained values are used then for all other centralities. The initial $P(V_n)$ distributions are broader than the unfolded ones only in the areas of relatively high flow values. The agreement of unfolded spectra with the data is very good. Since the unfolding suppresses strongly the non-flow fluctuations, Fig. 6 confirms the dynamical origin of the flow fluctuations in HYDJET++.

3. Conclusions

Anisotropic flow, azimuthal dihadron correlations and event-by-event fluctuations of the flow harmonics in Pb+Pb collisions at $\sqrt{s_{\rm NN}} = 2.76$ TeV are studied within the hybrid hydro+jets model HYDJET++. Several features are observed. Hadrons, produced in jet fragmentation, display very weak flow because of the jet quenching effect. These hadrons dominate particle spectrum at certain $p_{\rm T}$; the heavier the particle, the larger the transverse momentum. Such an interplay of soft and hard processes explains (i) the breaking of mass ordering of $p_{\rm T}$ distributions

of anisotropic flow; (ii) the falloff of the flow harmonics at intermediate transverse momenta; (iii) violation of the NCQ scaling at LHC energies compared to RHIC ones, because hard processes become more abundant with rising collision energy. The cross-talk of two harmonics, v_2 and v_3, leads to (i) long-range azimuthal dihadron correlations (ridge); (ii) formation of the characteristic double-hump structure at the away side; (iii) nonlinear contributions to higher order harmonics, e.g., to hexagonal flow, which is correlated with the triangular flow in central collisions and becomes more correlated with the elliptic flow in more peripheral ones. Analysis of EbyE flow fluctuations by means of the unfolding procedure reveals their dynamical nature in HYDJET++. Its origin is traced to the correlations between the coordinates and momenta of the hadrons and the velocities of the fluid cells.

Acknowledgments
LB acknowledges financial support of the Alexander von Humboldt Foundation.

References

[1] Lokhtin I P, Malinina L V, Petrushanko S V, Snigirev A M, Arsene I and Tywoniuk K 2009 *Comput. Phys. Commun.* **180** 779
[2] Amelin N S, Lednicky R, Pocheptsov T A, Lokhtin I P, Malinina L V, Snigirev A M, Karpenko Iu A and Sinyukov Yu M 2006 *Phys. Rev.* C **74** 064901
[3] Amelin N S, Lednicky R, Lokhtin I P, Malinina L V, Snigirev A M, Karpenko Iu A, Sinyukov Yu M, Arsene I and Bravina L V 2008 *Phys. Rev.* C **77** 014903
[4] Kisiel A, Taluc T, Broniowski W and Florkowski W 2006 *Comput. Phys. Commun.* **174** 669
[5] Lokhtin I P and Snigirev A M 2006 *Eur. Phys. J.* C **46** 211
[6] Sjostrand T, Mrenna S and Skands P Z 2006 *J. High Energy Phys.* JHEP05(2006)026
[7] Lokhtin I P, Belyaev A V, Malinina L V, Petrushanko S V, Rogochaya E R and Snigirev A M 2012 *Eur. Phys. J.* C **72** 2045
[8] Bravina L V, Brusheim Johansson B H, Eyyubova G Kh, Korotkikh V L, Lokhtin I P, Malinina L V, Petrushanko S V, Snigirev A M and Zabrodin E E 2014 *Eur. Phys. J.* C **74** (2014) 2807
[9] Voloshin S and Zhang Y 1996 *Z. Phys.* C **70** 665
[10] Poskanzer A M and Voloshin S A 1998 *Phys. Rev.* C **58** 1671
[11] Eyyubova G Kh, Korotkikh V L, Lokhtin I P, Petrushanko S V, Snigirev A M, Bravina L V and Zabrodin E E 2015 *Phys. Rev.* C **91** 064907
[12] Lokhtin I P, Belyaev A V, Eyyubova G Kh, Ponimatkin G and Pronina E Yu 2016 Charmed meson production pattern in PbPb collisions at the LHC *Preprint* hep-ph/1601.00799
[13] Bravina L V, Fotina E S, Korotkikh V L, Lokhtin I P, Malinina L V, Nazarova E N, Petrushanko S V, Snigirev A M and Zabrodin E E 2015 *Eur. Phys. J.* C **75** 588
[14] G. Eyyubova G, Bravina, Korotkih V L, Lokhtin I P, Malinina L V, Petrushanko S V, Snigirev A M and Zabrodin E 2009 *Phys. Rev.* C **80** 064907
[15] Zabrodin E E, Bravina L V, Eyyubova G Kh, Lokhtin I P, Malinina L V, Petrushanko S V and Snigirev A M 2010 *J. Phys.* G **37** 094060
[16] Zabrodin E E, Bravina L V, Brusheim Johansson B H, Crkovská J, Eyyubova G Kh, Korotkikh V L, Lokhtin I P, Malinina L V, Petrushanko S V and Snigirev A M 2016 *J. Phys.: Conf. Ser.* **668** 012099
[17] Crkovská J *et al* Influence of jets and final-state interactions on the triangular flow in ultrarelativistic heavy-ion collisions 2016 *Preprint* hep-ph/1603.09621
[18] Noferini F *et al* (ALICE Collaboration) 2013 *Nucl. Phys.* A **904-905** 438c
[19] Bravina L, Brusheim Johansson B H, Eyyubova G and Zabrodin E 2013 *Phys. Rev.* C **87** 034901
[20] Bravina L V, Brusheim Johansson B H, Eyyubova G Kh, Korotkikh V L, Lokhtin I P, Malinina L V, Petrushanko S V, Snigirev A M and Zabrodin E E 2014 *Phys. Rev.* C **89** 024909
[21] Aad G *et al* (ATLAS Collaboration) 2012 *Phys. Rev.* C **86** 014907
[22] Jia J *et al* (ATLAS Collaboration) 2013 *Nucl. Phys.* A **910-911** 276
[23] Adare A *et al* (PHENIX Collaboration) 2008 *Phys. Rev.* C **78** 014901
[24] Aamodt K *et al* (ALICE Collaboration) 2011 *Phys. Rev. Lett.* **107** 032301
[25] Alver B and Roland G 2010 *Phys. Rev.* C **81** 054905
[26] Aad G *et al* (ATLAS Collaboration) 2013 *J. High Energy Phys.* JHEP11(2013)183
[27] Adye T 2011 Unfolding algorithms and tests using RooUnfold *Preprint* physics.data-an/1105.1160